Electrostatics of Cell Membrane Recognition: Structure and Activity of Neutral and Cationic Rigid Push-Pull Rods in Isoelectric, Anionic, and Polarized Lipid Bilayer Membranes

Naomi Sakai,* David Gerard, and Stefan Matile*

Contribution from the Department of Organic Chemistry, University of Geneva, CH-1211 Geneva, Switzerland

Received August 22, 2000

Abstract: Design, synthesis, and structural and functional studies of rigid-rod ionophores of different axial electrostatic asymmetry are reported. The employed design strategy emphasized presence of (a) a rigid scaffold to minimize the conformational complexity, (b) a unimolecular ion-conducting pathway to minimize the suprastructural complexity and monitor the function, (c) an extended fluorophore to monitor structure, (d) variable axial rod dipole, and (e) variable terminal charges to create axial asymmetry. Studies in isoelectric, anionic, and polarized bilayer membranes confirmed a general increase in activity of uncharged rigid push-pull rods in polarized bilayers. The similarly increased activity of cationic rigid push-pull rods with an electrostatic asymmetry comparable to that of α-helical bee toxin melittin (positive charge near negative axial dipole terminus) is shown by fluorescence-depth quenching experiments to originate from the stabilization of transmembrane rod orientation by the membrane potential. The reduced activity of rigid push-pull rods having an electrostatic asymmetry comparable to that in α-helical natural antibiotics (a positive charge near the positive axial dipole terminus) is shown by structural studies to originate from rod "ejection" by membrane potentials comparable to that found in mammalian plasma membranes. This *structural* evidence for cell membrane recognition by asymmetric rods is unprecedented and of possible practical importance with regard to antibiotic resistance.

Introduction

Why is melittin a toxin and magainin 2 a natural antibiotic?[1] Both are α-helical cationic polypeptides that act by mediating ion transport across bilayer membranes (Figure 1). They share central structural characteristics: A semirigid "rod" of a length sufficient to span the hydrophobic core of bilayer membranes and facial amphiphilicity for self-assembly into transmembrane (TM) bundles with central hydrophilic channels. They differ, however, in axial electrostatic asymmetry. The positively charged amino acid residues are accumulated near the negative end of the axial rod dipole in melittin and near the positive dipole terminus in magainin. Following Merrifields original suggestion,[2] these two simplified situations of electrostatic rod asymmetry are referred to as "melittin-like" and "magainin-like".[3]

The importance of appropriate length and facial amphiphilicity for ion transport activity has been exemplified extensively with many natural and artificial molecular rods.[4,5] Elucidation of the importance of electrostatic rod asymmetry for cell membrane recognition proved more difficult. Nevertheless, it is possible to extract a simplified, tentative recognition mechanism from pertinent discussions in recent reports on this topic (Figure 2).[1−3,6−8] The key characteristic of this mechanism is that the formation of host−guest complex **1** with magainin-like rods in bacteria-type membranes with a high inside negative potential (ca. −200 mV)[7a] requires TM cation translocation for favorable axial dipole alignment (Figure 2, arrow a). Reduced

(1) Sakai, N.; Matile, S. *Chem. Eur. J.* **2000**, *6*, 1731−1737 and references therein.

(2) Juvvadi, P.; Vunnam, S.; Merrifield, R. B. *J. Am. Chem. Soc.* **1996**, *118*, 8989−8997 and references therein.

(3) Note that the terms magainin-like and melittin-like axial rod asymmetry are defined here as "excess positive charge near the positive dipole terminus" and "excess positive charge near the negative dipole terminus", respectively. Particularly, the example of magainin 2 illustrates clearly that, for example, (a) poor charge localization and (b) contributions of negative charges near negative the axial dipole terminus may not be negligible in future, refined definitions.[2,8,21]

(4) Recent references on peptide-based artificial ion channels and channel models: (a) Baumeister, B.; Sakai, N.; Matile, S. *Angew. Chem., Int. Ed.* **2000**, *39*, 1955−1958. (b) Schrey, A.; Vescovi, A.; Knoll, A.; Rickert, C.; Koert, U. *Angew. Chem., Int. Ed.* **2000**, *39*, 900−902. (c) Dieckmann, G. R.; Lear, J. D.; Zhong, Q.; Klein, M. L.; DeGrado, W. F.; Sharp, K. A. *Biophys. J.* **1999**, *76*, 618−630. (d) Clark, T. D.; Buehler, L. K.; Ghadiri, M. R. *J. Am. Chem. Soc.* **1998**, *120*, 651−656. (e) Lear, J. D.; Schneider, J. P.; Kienker, P. K.; DeGrado, W. F. *J. Am. Chem. Soc.* **1997**, *119*, 3212−3217. (f) Voyer, N.; Potvin, L.; Rousseau, E. *J. Chem. Soc., Perkin Trans. 2* **1997**, 1469−1472. (g) Meillon, J.-C.; Voyer, N. *Angew. Chem., Int. Ed. Engl.* **1997**, *36*, 967−969.

(5) Selected reviews on nonpeptide ion channels and channel models: (a) Kobuke, Y. In *Advances in Supramolecular Chemistry*; Gokel, G. W., Ed.; JAI: Greenwich, London, 1997, Vol. 4, 163−210. (b) Koert, U.; *Chem. Unserer Z.* **1997**, *31*, 20−26. (c) Gokel, G. W.; Murillo, O. *Acc. Chem. Res.* **1996**, *29*, 425−432. Recent references: (d) Renkes, T.; Schäfer, H. J. Siemens, P. M.; Neumann, E. *Angew. Chem., Int. Ed.* **2000**, *39*, 2512−2516. (e) Forman, S. L.; Fettinger, J. C.; Pieraccini, S.; Gottarelli, G.; Davis, J. T. *J. Am. Chem. Soc.* **2000**, *122*, 4060−4067. (f) Otto, S.; Janout, V.; DiGiorgio, A. F.; Young, M. C.; Regen, S. L. *J. Am. Chem. Soc.* **2000**, *122*, 1200−1204. (g) Pérez, C.; Espínola, C. G.; Foces-Foces, C.; Núñez-Coello, P.; Carrasco, H.; Martín, J. D. *Org. Lett.* **2000**, *2*, 1185−1188. (h) Kobuke, Y.; Nagatani, T. *Chem. Lett.* **2000**, 298−299. (i) Das, S.; Kurcok, P.; Jedlinski, Z.; Reusch, R. N. *Macromolecules* **1999**, *32*, 8781−8785. (j) Abel, E.; Maguire, G. E. M.; Murillo, O.; Suzuki, I.; De Wall, S. L.; Gokel, G. W. *J. Am. Chem. Soc.* **1999**, *121*, 9043−9052. (k) Qi, Z.; Sokabe, M.; Donowaki, K.; Ishida, H. *Biophys. J.* **1999**, *76*, 631−641. (l) Hall, C. D.; Kirkovits, G. J.; Hall, A. C. *Chem. Commun.* **1999**, 1897−1898. (m) Fritz, M. G.; Walde, P.; Seebach, D. *Macromolecules* **1999**, *32*, 574−580. Compare also: (n) Fyles, T. M.; Look, D.; Zhou, X. *J. Am. Chem. Soc.* **1998**, *120*, 2997−3003. (o) Nolte, R. J. M. *Chem. Soc. Rev.* **1994**, 11−19.

10.1021/ja003141+ CCC: $20.00
Published on Web 02/22/2001

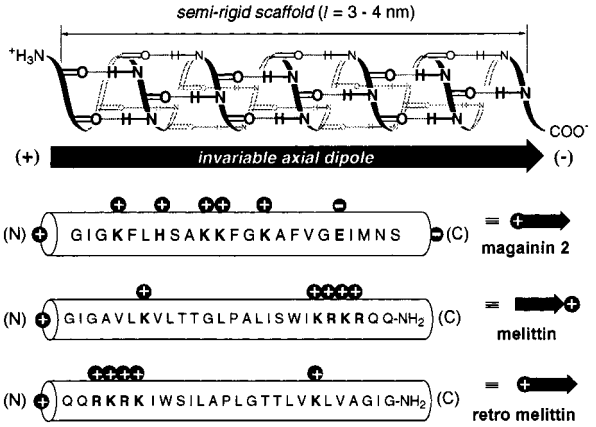

Figure 1. Above: uniform alignment of the backbone carbonyl dipoles accounts for the inherent, invariable axial dipole of α-helical membrane-spanning peptides. Below: schematic diagrams for axial electrostatic asymmetry, structure, and charge distribution for antibiotic magainin 2, toxic melittin, and synthetic retro melittin in α-helical conformation. One-letter abbreviations are used for amino acids.

toxicity to mammals may, thus, originate from insufficient polarization of mammalian plasma membranes to promote such charge translocation. Because reversed TM rod orientation is unlikely due to destructive dipole−potential interactions (Figure 2, arrow b), an inactive host−guest complex **2** may result for magainin-like rods in mammal-type membranes. The formation of active host−guest complexes **3** and **4** in the unpolarized membranes that are frequently used in biophysical model systems, however, is conceivable for rods with magainin- and melittin-like axial asymmetry.[8] Preferential TM orientation of melittin-like rods in unpolarized (i.e., **4**), mammal-type (i.e., **5**) and bacteria-type bilayer membranes (i.e., **6**) is consistent with poor cell membrane recognition (i.e., toxicity).[1]

Insightful studies from the Merrifield lab provided persuasive support for the simplified recognition mechanism depicted in Figure 2.[2] Retro melittin, for example, was shown to exhibit reduced hemolytic, but maintained antibiotic, activity as compared to isomeric melittin. Because retro melittin is characterized

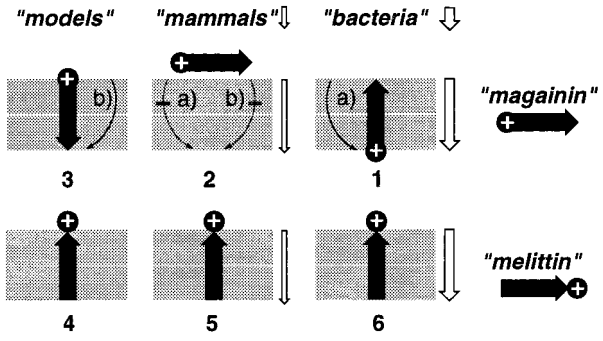

Figure 2. Tentative cell membrane recognition mechanism of molecular rods with axial electrostatic asymmetry.[1−3,6−8] Emphasis is on the electrostatic interactions between rods and membrane potential:[6] rods with magainin-[8] (top) and melittin-like asymmetry (bottom) on one side and unpolarized bilayer membranes common in model systems (left), weakly polarized bilayer membranes similar to mammalian plasma membranes (center), and highly polarized bilayer membranes similar to bacterial plasma membranes (right) on the other. (a) TM rod orientation, including TM cation translocation. (b) TM rod orientation, excluding TM cation translocation. Schematic diagrams for electrostatic rod asymmetry are as defined in Figure 1 and Table 1 (forward block arrow, axial rod dipole;[3] forward open arrow, direction of mammalian membrane potential (up to −150 mV); forward open arrow, direction of bacterial membrane potential (ca. −200 mV). Arrows, except a and b, are pointing from plus to minus. Hydrophobic cores of lipid bilayers are in gray.

by magainin-like electrostatic asymmetry (Figure 1), selective formation of inactive complex **2** in weakly, and active complex **1** in highly, polarized membranes is conceivable to account for cell membrane recognition by retro melittin (Figure 2). Recent reports dealing with antibiotic activity of cationic helical β-peptides[9] underscored that a better understanding of cell membrane recognition by electrostatic fine-tuning may, indeed, provide rational design strategies for novel antibacterials having promising properties concerning antibiotic resistance.[1,2,7]

Despite high scientific and commercial interest in the antibiotic activity of magainin-like rods, insights into the electrostatic principles underlying their recognition mechanism remain elusive on the molecular structural level.[1] In other words, it turns out to be very difficult to actually "see" the membrane potential-induced rod reorientations assumed in host−guest complexes **1**−**3** (Figure 2). We have suggested recently that fluorescent, ionophoric rigid *p*-octiphenyl rods may be of use to elucidate the subtle balance of constructive and destructive electrostatic interactions underlying cell membrane recognition.[1] This concept emerged from a preliminary model study with rigid push-pull rod **7** (Figure 3).[10] *p*-Octiphenyl **7** comprises four lateral azacrowns to mediate TM ion transport, a terminal π-donor and a terminal π-acceptor, to provide a permanent axial rod dipole. Asymmetric rod **7** was shown to depolarize polarized bilayer membrane more efficiently than the symmetric rod **8**, which has a nearly identical global structure. On the basis of these results, five design principles have been elaborated for the construction of "universal" probes for comprehensive clarification of the electrostatic principles underlying cell membrane recognition:[1] (1) a rigid scaffold to minimize the conformational complexity, (2) a unimolecular TM ion-conducting pathway to simplify the suprastructural complexity and to monitor functions, (3) an extended fluorophore to monitor structures, (4) variable

(6) With respect to results described in this work, the tentative recognition mechanism in Figure 2 emphasizes stabilization of TM rods by favorable alignment of the rod dipole to inside negative membrane potentials and neglects contributions from multivalent (compare, e.g., (a) Mammen, M.; Choi, S.-K.; Whitesides, G. M. *Angew. Chem., Int. Ed.* **1998**, *37*, 2754−2794) interfacial ion pair formation between anionic lipid headgroups and cationic rod charges. Further simplifications include the exclusion of tilted rods, partial rod insertions, mixed populations, membrane composition and phase behavior, and so on (compare, e.g., (b) Schanck, P. J.; Lins, L.; Brasseur, R. *J. Theor. Biol.* **1999**, *198*, 173−181).

(7) (a) Gabay, J. E. *Science* **1994**, *264*, 373−374, other articles in this special issue of *Science*, and references therein. Recent review: (b) Kourie, J. I.; Shorthouse, A. A. *Am. J. Physiol. Cell Physiol.* **2000**, *278*, C1063−C1087. For alternative approaches to cell membrane recognition focusing on their molecular composition, phase behavior, thickness, and so on, see, for example: (c) Breukink, E.; Wiedemann, I.; van Kraaij, C.; Kuipers, O. P.; Stahl, H.-G.; de Kruijff, B. *Science* **1999**, *286*, 2361−2364. (d) Bolard, J. *Biochim. Biophys. Acta* **1986**, *864*, 257−304, and references therein, in refs 1 and 5f.

(8) Note that the orientation of magainin 2 itself in unpolarized membranes is presumably not TM, as in **3**, but is interfacial, as in **2** (compare, e.g., (a) Matsuzaki, K.; Murase, O.; Tokuda, H.; Funakoshi, S.; Fujii, N.; Miyajima, K. *Biochemistry* **1994**, *33*, 3342−3349. (b) Matsuzaki, K. *Biochim. Biophys. Acta* **1999**, *1462*, 1−10). This alternative structure of **3** with interfacial magainin 2 is, however, in excellent agreement with the mechanism in Figure 2, because magainin 2 contains two anions near the negative dipole terminus in addition to multiple cations near the positive dipole terminus. Disfavored TM transfer of these terminal anions may, thus, account for interfacial magainin 2 with reduced activity in unpolarized membranes. Studies with the corresponding push-pull rods with one anionic and one cationic terminus are ongoing.

(9) (a) Porter, E. A.; Wang, X.; Lee, H. S.; Weisblum, B.; Gellman, S. H.; *Nature* **2000**, *404*, 565−565. (b) Hamuro, Y.; Schneider, J. P.; DeGrado, W. F. *J. Am. Chem. Soc.* **1999**, *121*, 12200−12201.

(10) (a) Winum, J.-Y.; Matile, S. *J. Am. Chem. Soc.* **1999**, *121*, 7961−7962. (b) Supporting Information of 10a.

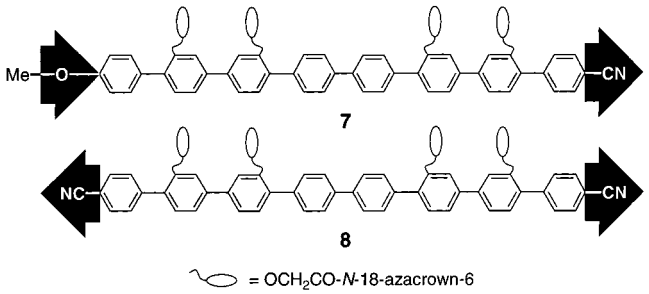

Figure 3. Structure of neutral rigid push-pull rod **7** and symmetric pull-pull rod **8**.

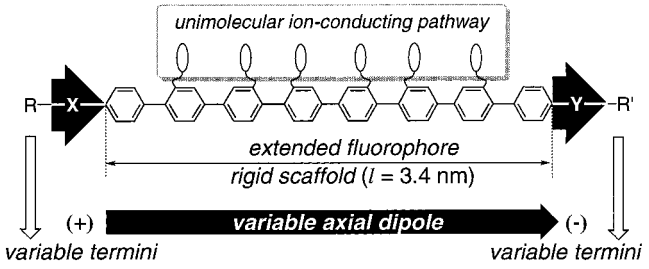

Figure 4. Design principles for rigid-rod ionophores with variable axial electrostatic asymmetry.

axial rod dipole, and (5) variable terminal charges to precisely tune axial electrostatic asymmetry (Figure 4).

The call for rigid-rod scaffolds, extended fluorophores and variable axial rod dipoles was of particular interest, because these structural characteristics are incompatible with α-helical peptides and were apparently unique for rods **7** and **8** until now.

Here we report the synthesis and study of a neutral push-pull rod (**10**), cationic push-pull rods with magainin- (**14**) and melittin-like (**13**) electrostatic asymmetry, and the corresponding neutral (**9**, **11**) and cationic (**12**, **15**) *p*-octiphenyl ionophores without axial dipole (Scheme 1 and Table 1). Functional and structural studies in isoelectric, anionic, and polarized bilayer membranes under comparable conditions are described to afford unprecedented insights into the molecular structural level of membrane recognition by electrostatically asymmetric rods.

Results and Discussion

Design. As described for model rods **7** and **8** (Figure 3),[10] the design of rigid-rod ionophores **9**−**20** focused on a rigid scaffold, a unimolecular ion-conducting pathway, and an extended fluorophore, as well as variable axial rod dipole and terminal charges, to create axial asymmetry (vide supra, Figure 4).[1] In contrast to **7** and **8**, ionophores **9**−**20** contain six instead of four lateral azacrowns. This change was made to improve the unimolecular TM ion-conducting pathway (Scheme 1 and Table 1).[4f,g,5a−c,j,l,o] Moreover, the terminal π-donors and π-acceptors in **7** and **8** were replaced by sulfides and sulfones. This second change was necessary for the attachment of cationic side chains to the terminal π-donors and acceptors. Facile synthetic access to variable cationic termini was crucial for, for example, functional and structural studies with push-pull rods with melittin- (**13**) and magainin-like electrostatic asymmetry (**14**).

Synthesis. Rigid-rod molecules **9**−**20** were prepared from *p*-sexiphenyl **21** (Scheme 1). Suzuki-coupling[11] with equimolar amounts of sulfides **22** and **23** and separation of the product mixture by semipreparative RP-HPLC (reverse-phase high-pressure liquid chromatography) afforded push-push rods **9**, **17**, and **16** in excellent 15%, 31%, and 15% yield, respectively. Deiodinated *p*-septiphenyls were observed as minor side products (overall, 11%).

Among multiple methods for sulfide oxidation,[12] the following conditions were selected on the basis of qualitative model studies with sulfide **24** (Scheme 2). Initial partial oxidation with *m*CPBA yielded almost quantitative formation of sulfoxide **25** in addition to sulfide **24**. Subsequent oxidation of this mixture with $KMnO_4$[12b] selectively converted sulfoxide **25** into sulfone **26** with nearly negligible oxidation of sulfide **24**. The remaining sulfoxide **25** that was obtained from the incomplete oxidation could be selectively reduced with TFAA/NaI[12c] to ultimately give a 1:1 mixture of sulfide **24** and sulfone **26**.

Application of the three-step protocol in Scheme 2 to the symmetric disulfide **9** yielded a clean mixture of push-push rod **9**, push-pull rod **10**, and pull-pull rod **11** that was readily separated by semipreparative RP-HPLC. The same procedure was also compatible with the more complex situation of asymmetric push-push rod **17**. The four desired rods **17**−**20** could be separated and isolated in excellent yield by semipreparative RP-HPLC; deprotection with TFA gave the cationic rigid-rod ionophores **12**−**15**.

During the interpretation of the usual data collected to confirm the correct structure of all new compounds (see Supporting Information), we observed peculiar multiple satellites in the ESI-MS (electrospray ionization mass spectrometry) of cationic rigid-rod ionophores (Figure 5). As illustrated for melittin-like push-pull rod **13**, dominant molecular ion peaks with two or three sodium cations were followed by several smaller signals with constant additional *m*/*z* corresponding to the sodium salt of TFA. This finding, thus, unexpectedly illustrated the capacity of rigid-rod ionophores to bind multiple cations and, thus, (possibly) mediate TM ion transport by the same cation "hopping" or "wire" mechanism that emerges as crucial for functional ion-conducting pathways in biological ion channels.[13,14]

The previously communicated synthesis of *p*-sexiphenyl **21** from biphenyl crowns **27** and **28** turned out to be less practical than the route through "insoluble" *p*-sexiphenyl **29**, prepared directly from bianisoles **30** and **31**, and solubilized[14] *tert*-butyl ester **32** (Scheme 3, see Supporting Information for discussion).[15] Subunit **22** leading to the cationic rod termini in **12**−**15** was prepared from amine **33** (Scheme 4). BOC protection (to give bromide **34)** and condensation with arylthiol **35** gave bromide **36** that was converted into boronate **22**.

Ion Transport Activity of Neutral and Cationic Rods in Unpolarized Bilayer Membranes. The capacity of rods **9**−**15** to mediate ion transport across unpolarized bilayer membranes with isoelectric, zwitterionic surfaces was assessed using uniformly sized EYPC (egg yolk phosphatidylcholine)-SUVs (small unilamellar vesicles) with internal pH-sensitive fluorescent probe HPTS (8-hydroxypyrene-1,3,6-trisulfonic acid, trisodium salt) (Figure 6).[17] A TM pH gradient of $\Delta pH \approx 1.0$

(11) (a) Suzuki, A. *J. Organomet. Chem.* **1999**, *576*, 147−168. (b) Murata, M.; Watanabe, S.; Masuda, Y. *J. Org. Chem.* **1997**, *62*, 6458−6459. (c) Ishiyama, T.; Murata, M.; Miyama, N. *J. Org. Chem.* **1995**, *60*, 7508−7510.

(12) (a) Uemura, S. *Comprehensive Organic Synthesis*; Trost, B. M., Ed.; Pergamon Press: Oxford, 1991; Vol. 6, pp 757−787. (b) Henbest, H. B.; Khan, S. A. *J. Chem. Soc., Chem. Commun.* **1968**, 1036−1036. (c) Drabowicz, J.; Oae, S. *Synthesis* **1977**, 404−405.

(13) (a) Aqvist, J.; Luzhkov, V. *Nature* **2000**, *404*, 881−884. (b) Doyle, D. A.; Morais Cabral, J.; Pfuetzner, R. A.; Kuo, A.; Gulbis, J. M.; Cohen, S. L.; Chait, B. T.; MacKinnon, R. *Science* **1998**, *280*, 69−77. (c) Gulbis, J. M.; Zhou, M.; Mann, S.; MacKinnon, R. *Science* **2000**, *289*, 123−127.

(14) Sakai, N.; Majumdar, N.; Matile, S. *J. Am. Chem. Soc.* **1999**, *121*, 4294−4295.

(15) Robert, F.; Winum, J.-Y.; Sakai, N.; Gerard, D.; Matile, S. *Org. Lett.* **2000**, *2*, 37−39.

Scheme 1[a]

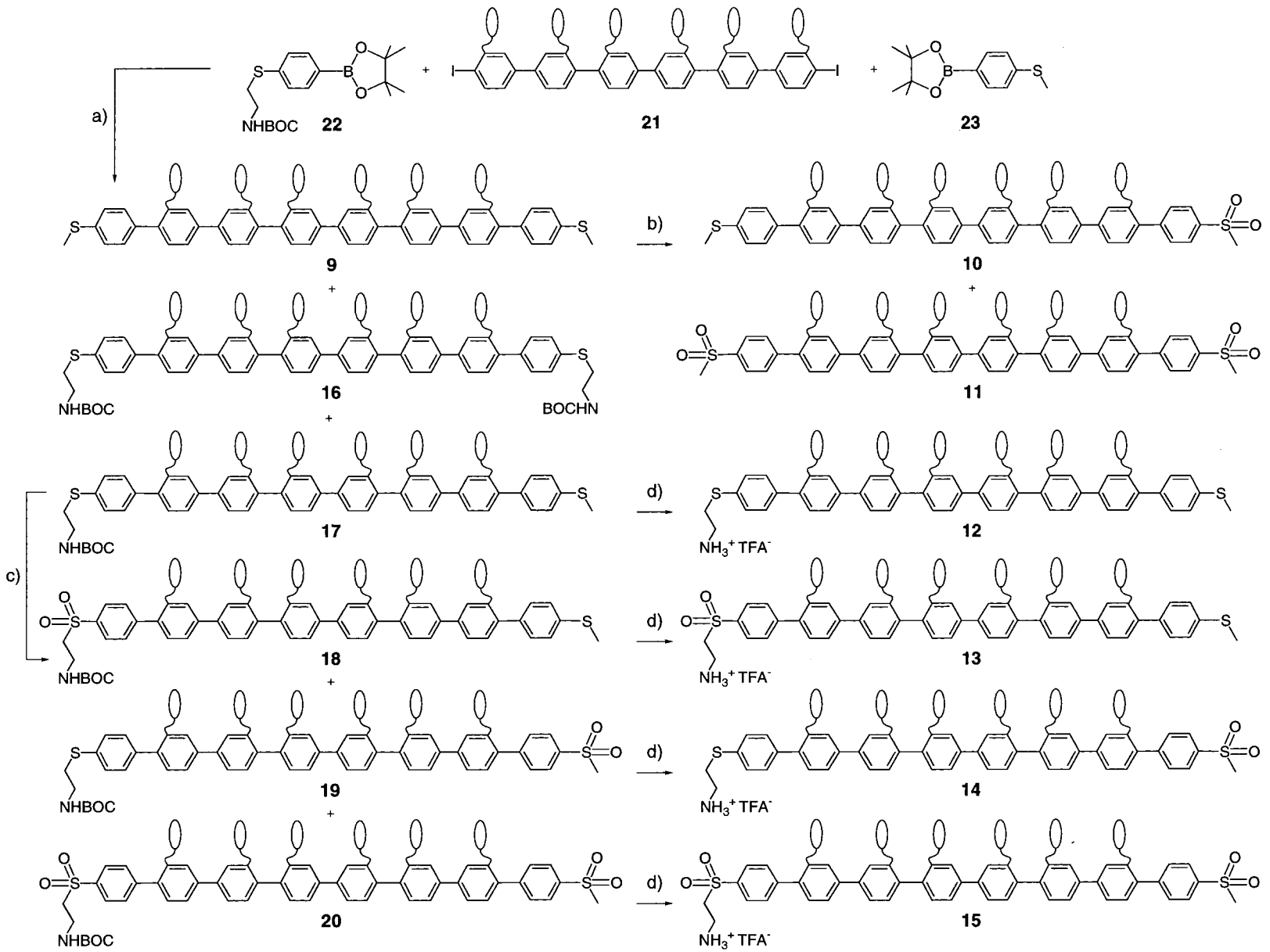

[a] (a) $PdCl_2$(dppf), Na_2CO_3; isolated 15% (**9**), 31% (**17**), 15% (**16**). (b) 1, *m*CPBA; 2, $KMnO_4$, $MgSO_4$; 3, TFAA/NaI; isolated 26% (**11**), 40% (**10**), 31% (**9**). (c) 1, *m*CPBA; 2, $KMnO_4$, $MgSO_4$; 3, TFAA/NaI; isolated 25% (**20**), 25% (**19**), 22% (**18**), 23% (**17**). (d) TFA, 90% (**12**), 71% (**13**), 89% (**14**), 91% (**15**). Lateral rod substitution as in Scheme 3.

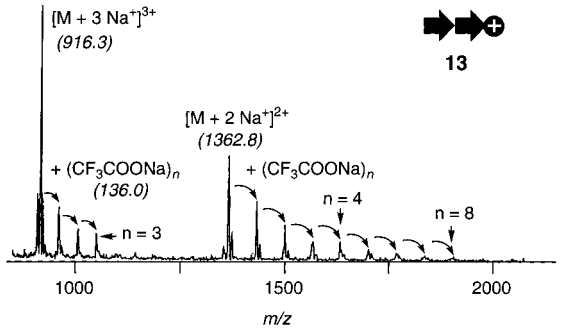

Figure 5. ESI-MS (MeOH) of cationic rigid push-pull rod **13**.

Table 1. Schematic Diagrams for the Electrostatic Asymmetry of Rigid-Rod Ionophores Described in This Study (Scheme 1)

compound		X	Y	R	R'
9		S	S	$-CH_3$	$-CH_3$
10		S	SO_2	$-CH_3$	$-CH_3$
11		SO_2	SO_2	$-CH_3$	$-CH_3$
12		S	S	$-CH_3$	$-NH_3^+$
13		S	SO_2	$-CH_3$	$-NH_3^+$
14		S	SO_2	$-NH_3^+$	$-CH_3$
15		SO_2	SO_2	$-CH_3$	$-NH_3^+$
16	(BOC) (BOC)	S	S	-NHBOC	-NHBOC
17	(BOC)	S	S	$-CH_3$	-NHBOC
18	(BOC)	S	SO_2	$-CH_3$	-NHBOC
19	(BOC)	S	SO_2	-NHBOC	$-CH_3$
20	(BOC)	SO_2	SO_2	$-CH_3$	-NHBOC

Scheme 2

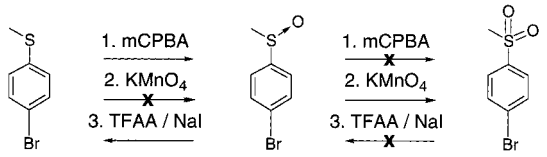

was established by the increase of the external pH using base. The ionophores were added at time 0 and the rate of pH gradient collapse was monitored by following the excitation and emission intensity of internal HPTS as a function of time (Figure 6).[18]

(16) Dourtoglou, V.; Gross, B. *Synthesis*, **1984**, 572−574.

(17) Weiss, L. A.; Sakai, N.; Ghebremariam, B.; Ni, C.; Matile, S. *J. Am. Chem. Soc.* **1997**, *119*, 12142−12149.

(18) Note that this interpretation is only valid because HPTS efflux can be excluded (compare section on lytic activity). When compared to other pH-sensitive probes such as CF, the advantage of HPTS is compatibility with double-channel fluorescence kinetics. In these experiments, fluorescence intensity change was simultaneously monitored at another wavelength (λ_{em} = 510 nm, λ_{ex} = 405 nm) to identify and eliminate possible changes in emission that do not originate from changes in pH (compare: Haugland, R. P. *Handbook of Fluorescent Probes and Research Chemicals*; 6th ed, Molecular Probes: Eugene, OR, 1996). However, influence from the fluorescence of the rods was much greater in this channel; thus, the ratiometric normalization was not applied.

Scheme 3[a]

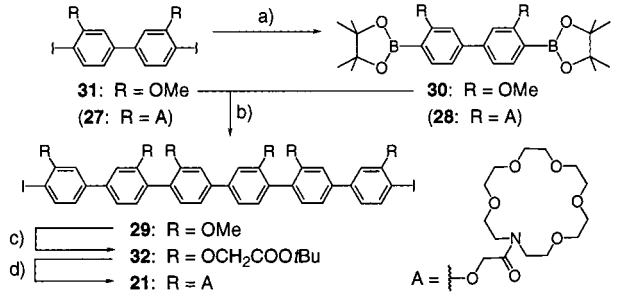

[a] (a) 4,4,5,5-tetramethyl-[1,3,2]-dioxaborolane,[11c] $PdCl_2$(dppf), 69%. (b) $Pd(PPh_3)_4$, Na_2CO_3, 10%. 1, BBr_3; 2, *tert*-butylbromoacetate, Cs_2CO_3, 84%. (d) 1, TFA/CH_2Cl_2; 2, 18-azacrown-6, HBTU, Et_3N, 69% (revised from ref 15).

Scheme 4[a]

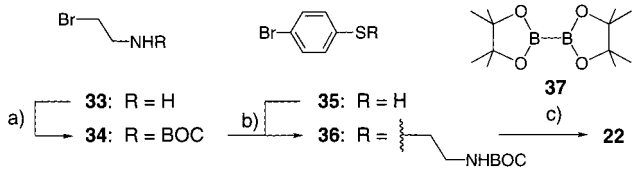

[a] (a) BOC_2O, 84%. (b) K_2CO_3, 87%. (c) bis(pinacolato)diboron, $PdCl_2$(dppf), 47% (conversion yield, 61%).[11c]

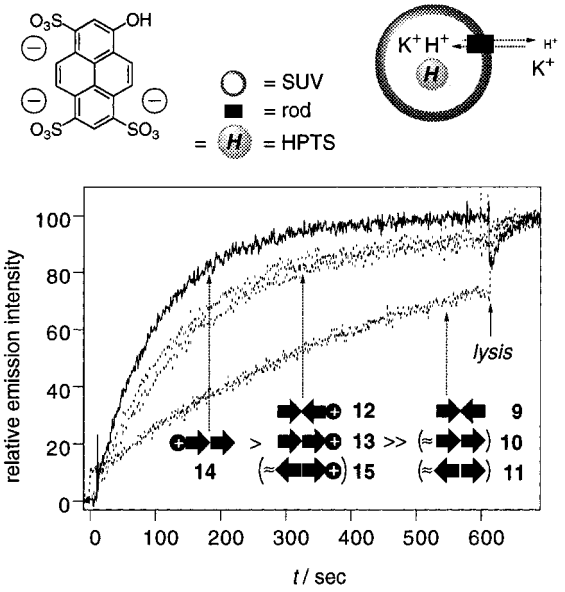

Figure 6. Assay for ion transport activity of neutral and cationic rods in unpolarized bilayer membranes:[17,18] top, schematic representation of the assay; bottom, changes in fluorescence intensity of intravesicular HPTS after ionophore (10 μM) addition as a function of time (relative emission intensity = $(I_t - I_0)/(I_\infty - I_0) \times 100\%$; λ_{em} = 510 nm, λ_{ex} = 460 nm). Complete lysis (I_∞) was achieved by excess Triton X-100 or melittin[17] (0.25 mM EYPC-SUVs in 10 mM potassium phosphate buffer, 100 mM KCl). Curves for rods given in parentheses were identical to those of the parent compound and are not shown for clarity.

Compared to the previous model rods **7** and **8** (Figure 3),[10] the activity of the corresponding neutral rods **9**−**11** (Figure 4) was not substantially higher (Figure 6). This was surprising, because the presence of six instead of four lateral azacrowns was expected to result in increased activity. Our suspicion that relatively poor water-solubility and incorporation into bilayer membranes, rather than the number of lateral azacrowns, chiefly govern the activity of neutral rods **7**−**11** under these conditions was confirmed by the substantially increased activity of all cationic rods (**12**−**15**, Figure 6).

The highest activity was observed for magainin-like rod **14**. Structural studies suggested that this effect does not originate from improved incorporation or TM orientation (compare to section on structural studies). A likely explanation, thus, considers favorable influence of maximal global electrostatic asymmetry, as compared to all of the other rods (i.e., the sum of axial dipole plus terminal charges in rod **14**) on the properties of the adjacent ion-conducting pathway.[4e]

Nearly identical activities were observed for ion transport across unpolarized bilayer membranes having anionic surfaces prepared by doping EYPC-SUVs with 50% EYPG (egg yolk phosphatidylglycerol) (not shown). This suggested that, surprisingly,[1,2,7,8] constructive electrostatic interactions between the membrane surfaces and the rod termini are irrelevant for ion transport activity under these conditions. Multivalent interactions[6a] are presumably required for recognition of negatively charged membrane surfaces. Further studies with anionic membranes were, thus, redundant.

The concentration dependence of all of the observed flux rates in unpolarized SUVs was roughly linear (not shown). This trend is in support of the expected presence of monomeric active structures.[5f,4a,10b] No indications for rod self-assembly were seen during all of the reported structural and functional studies (compare, for example, ESI-MS in Figure 5) with one exception: all fluorescence kinetic measurement with pull-pull rods **11** and **15** were hampered by the occasional appearance of large noise. These peculiar observations, made with disulfone rods only, may stem from light scattering and, thus, originate from self-assembly of disulfone rods in water. Because of minor interest for studies of membrane recognition, this phenomenon was not further investigated, and studies of the interaction of disulfone rods with lipid bilayers were discontinued.

Ion Transport Activity of Neutral and Cationic Rods in Polarized Bilayer Membranes. Doubly labeled, polarized EYPC-SUVs with internal HPTS and external safranin O were prepared as described previously (Figure 7).[10] In brief, uniformly sized EYPC-SUVs were prepared by dialytic detergent removal using a buffer containing 100 mM K^+. External K^+ was subsequently exchanged with isoosmolar Na^+ by dialysis and gel filtration.[10b] An inside negative membrane potential was established by the addition of K^+ carrier valinomycin at concentrations sufficient for slow K^+ transport without rapid K^+ gradient collapse (Figure 7, background curve).[10b] Standard calibration of the emission intensity of the potential-sensitive dye safranin O indicated that the maximal potassium diffusion potentials obtained by this procedure were about −150 mV (corresponding to a relative emission intensity of 0 in Figure 7).[19b] This value indicated the presence of ∼300 μM residual external K^+. A maximal Nernst potential around −150 mV is comparable to highly polarized mammalian plasma membranes but below that of Gram-positive and -negative bacteria.[7a]

The capacity of ionophoric rods to depolarize these mammal-type bilayer membranes was reported by changes of safranin O emission as a function of time after addition (Figure 7).[10,19] In contrast to their roughly identical activity in unpolarized EYPC-SUVs, and despite their almost identical global structure, the capacity of neutral push-pull rod **10** to depolarize polarized membranes exceeded that of neutral push-push rod **9** clearly. This result was identical to that obtained previously for the neutral push-pull rod **7** and push-push rod **8** (Figure 3).[10] Favorable alignment of axial rod dipoles with membrane potentials appears, thus, to be, indeed, a general mechanism for cell membrane recognition, independent of the chemical nature of the terminal π-donor and π-acceptors and tolerant to modifications of the lateral ion-conducting pathway.

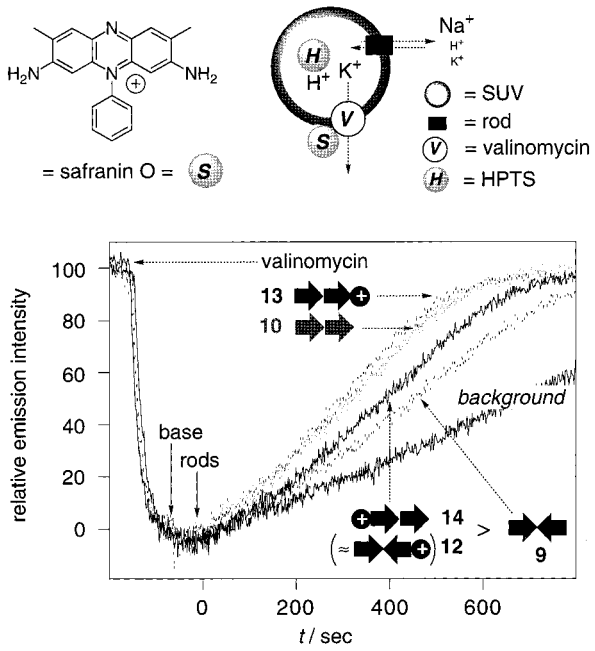

Figure 7. Assay for ion transport activity of neutral and cationic rods in polarized bilayer membranes:[10,19,20] top: schematic representation of the assay; bottom, changes in fluorescence intensity of extravesicular safranin O (10 μM) during the addition of valinomycin (0.6 μM, for membrane polarization), base (for ΔpH ≈ 1.0), rods (10 μM), and final complete depolarization (excess melittin). Relative emission intensity = $(I_t - I_0)/(I_\infty - I_0) \times 100\%$; $\lambda_{em} = 581$ nm, $\lambda_{ex} = 522$ nm. Relative emission intensity at 0% relates to a potential of about −150 mV, a relative emission intensity at 100% to 0 mV. (Conditions: 0.5 mM EYPC-SUVs with 10 mM potassium phosphate 100 mM KCl inside, in 10 mM sodium phosphate buffer, 100 mM NaCl.) Curves for rods given in parentheses were identical to those of the parent compound and are not shown for clarity.

In unpolarized EYPC-SUVs, cationic rods were generally more active than neutral rods (Figure 6). In polarized EYPC-SUVs, this trend did not hold (Figure 7). Only the cationic push-pull rod **13** with melittin-like electrostatic axial asymmetry exhibited the activity in the range of the neutral push-pull rod **10**. The most distinct decrease in activity was observed for magainin-like push-pull rod **14**, dropping from the highest activity in unpolarized membranes to the second-lowest activity in polarized membranes. Only the symmetric, neutral rod **9** remained less active than rod **14** with the highest global axial asymmetry.[20]

Structural Studies of Cationic Rigid Push-Pull Rods in Unpolarized and Polarized Bilayer Membranes. The activities of melittin-like rod **13** and magainin-like rod **14** in polarized and unpolarized membranes were consistent with the biological activities of the corresponding α-helical rods.[21] In contrast to the situation with their biological counterparts, elucidation of

(19) (a) Woolley, G. A.; Deber, C. M. *Biopolymers* **1989**, *28*, 267−272. (b) Singh, A. P.; Nicholls, P. *J. Biochem. Biophys. Methods* **1985**, *11*, 95−108.

(20) Control experiments demonstrated that valinomycin does not affect the ion transport activity of rods in EYPC-SUVs with H^+ but without K^+ and Na^+ gradients (for a discussion of this effect, see ref 17). The high sensitivity of this assay toward minimal changes in temperature, that is, highest importance for strict temperature control (25 ± 0.5°, using a thermostated sample holder) for successful studies, must be emphasized. For details on calibration of the assay with regard to valinomycin and safranin O concentration,[19] melittin experiments, and simultaneous pH-gradient detection using intravesicular HPTS by triple channel fluorescence kinetics, compare to ref 10b.

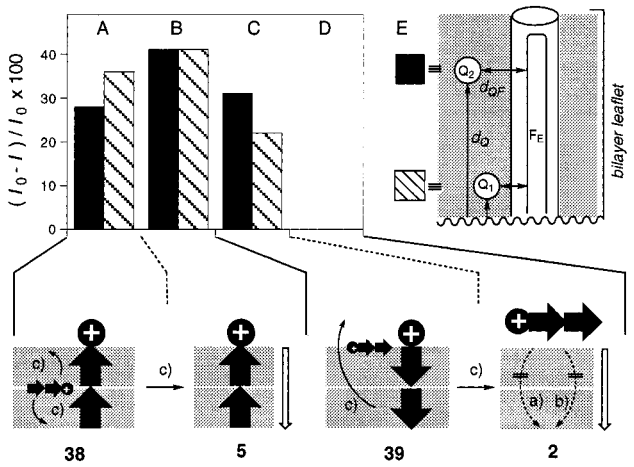

Figure 8. Assay for structural studies of cationic rods in unpolarized and polarized bilayer membranes.[17] Quenching of the emission of fluorescent rods **13** (A, B) and **14** (C, D) in unpolarized (A, C) and polarized EYPC-SUVs (B, D). Relative emission intensities $(I_0 - I)/I_0 \times 100\%$ were calculated from the emission of rods (0.1 μM) in unlabeled EYPC-SUVs (I_0, 0.25 mM) and EYPC-SUVs doped with 8.9 mol % of either 12-DOXYL-PC (Q_1) or 5-DOXYL-PC (Q_2). Inside negative potentials were applied with a K^+ gradient and valinomycin as described for function (Figure 7). Potential-induced structural changes (c) were not observed in the absence of valinomycin.

the structural basis of their bilayer membrane recognition mechanism under comparable experimental conditions was expected to be unproblematic using simplified fluorescence-depth quenching techniques in polarized and unpolarized EYPC-SUVs.[1]

The usefulness of extended rigid fluorophores to simplify structural studies in bilayer membranes by fluorescence-depth quenching at relevant concentrations has been demonstrated extensively.[1,4a,17] In brief, EYPC-SUVs were labeled with 8.9 mol % lipids containing a quencher either near the middle (i.e., a central quencher Q_1, $d_Q = 5.8$ Å) or near the surface of the bilayer (i.e., an interfacial quencher Q_2, $d_Q = 12.2$ Å) (Figure 8E). Measurement of the quenching efficiency by Q_1 and Q_2 on the emission of fluorescent rods in comparison to that in unlabeled EYPC-SUVs reveals central rod location for ($Q_1 \gg Q_2$)-efficiency, interfacial rods for ($Q_1 \ll Q_2$), and TM rods for ($Q_1 \approx Q_2$).[1]

In unpolarized EYPC-SUVs, quenching of melittin-like rod **13** and its isomer **14** varied between 23% and 34% and did not depend much on the location of the quencher (Figure 8A,C). Although this ($Q_1 \approx Q_2$)-situation was in general support of TM rod orientation, the small differences seen between central and interfacial quenchers were above experimental error (5%) and reproducible. According to parallax analysis,[22] these differences were, however, not sufficiently distinct to indicate interfacial or central rod location (6.9 Å for **13** and 11.2 Å for **14** from the center of the bilayer). The ($Q_1 \geq Q_2$) situation with melittin-like **13** may, thus, be best explained by the presence of a minor population of central rods in addition to a major population of TM rods (i.e., **38**, Figure 8A). The complementary ($Q_1 \leq Q_2$) situation with isomer **14** would then originate from the presence of minor interfacial populations in addition to mainly TM rods (i.e., **39**, Figure 8C). The presence of partially inserted or tilted rods can, however, not be fully excluded.[6b] Thus, although roughly consistent with the expectable host−guest complexes in unpolarized, isoelectric bilayer membranes (i.e., **4** and **3**, Figure 2), fluorescence-depth quenching results remained partially ambiguous and were suggestive of a more complex situation (i.e., **38** and **39**, Figure 8).

The application of an inside negative membrane potential by the identical method used for functional studies (Figure 7) had a profound effect on this comparably poor rod organization in unpolarized EYPC-SUVs (Figure 8c). A straightforward ($Q_1 = Q_2$) situation was induced for melittin-like **13** (Figure 8B). This fully corroborated favorable alignment of the TM axial rod dipole with mammal-type membrane potentials (i.e., host−guest complex **5**, Figures 2, 8). In sharp contrast, negligible quenching was observed for isomer **14** (Figure 8D). This proved, on the structural level, inhibition of TM orientation of magainin-like rods by mammal-type membrane potentials (i.e., host−guest complex **2**, Figures 2, 8) which confirms both unfavorable charge translocation (Figure 8a) and alignment of dipole with potential (Figure 8b).

The, thus far, unique variability of axial electrostatic asymmetry in rigid push-pull rods combined with their facile and reliable detectability in bilayer membranes, thus, revealed indeed valuable and novel insights into the structural basis of cell membrane recognition. Namely, increased activity of melittin-like rods **13** in polarized bilayers (Figures 6 and 7) was demonstrated to originate from the stabilization of TM rod orientation by inside negative potentials (Figure 8A,B). Reduced activity of magainin-like rods **14** in polarized membranes, on the other hand, was in excellent agreement with experimental structural evidence for voltage-induced inhibition of rod binding in TM orientation.

Lytic Activity of Neutral and Cationic Rods in Unpolarized Bilayer Membranes. The above studies provided unprecedented direct structural support that electrostatic rod asymmetry may account for, for example, the biological activity of the toxic melittin and the antibiotic magainins. Although consequently of minor importance for cell membrane recognition, the mechanism of ion transport by push-pull rigid-rod ionophores was, nevertheless, elucidated by dye leakage and planar bilayer conductance experiments (see Supporting Information). In view of the capacity of melittin and magainins to mediate transport of relatively large molecules across bilayer membranes, an assessment of lytic activity of the corresponding TM push-pull rods was of particular interest. For this reason, dye leakage from EYPC-SUVs loaded with CF (5(6)-carboxyfluorescein) at high, self-quenching concentrations was measured by monitoring changes in CF fluorescence as a function of time after the addition of ionophores **9**−**14** (Figure 9).[4a,17] Corroborating absence of lysis and TM pores >10 Å, no significant CF-efflux was detectable with all rods. These findings confirmed that cell membrane recognition and (hemo)lytic activity are, at least in this case,[2,9] unrelated.

Conclusions

The objective of this study was to assess the potential of rationally designed universal probes for comprehensive elucidation of the electrostatic principles underlying cell membrane recognition on the molecular structural level. Probe design emphasized the presence of an invariable rigid scaffold, a unimolecular ion-conducting pathway, and extended fluorophore in combination with systematically variable axial dipole and terminal charges. The above results demonstrate that this unique approach permits direct correlation of functional studies in unpolarized, anionic, and polarized bilayer membranes with straightforward structural studies under nearly identical conditions.

(21) For a comparison of these results with magainin 2 and other natural antibiotics, see: Kobayashi, S.; Takeshima, K.; Park, C. B.; Matsuzaki, K. *Biochemistry* **2000**, *39*, 8648−8654.

(22) Abrams, F. S.; London, E. *Biochemistry* **1992**, *31*, 5312−5322.

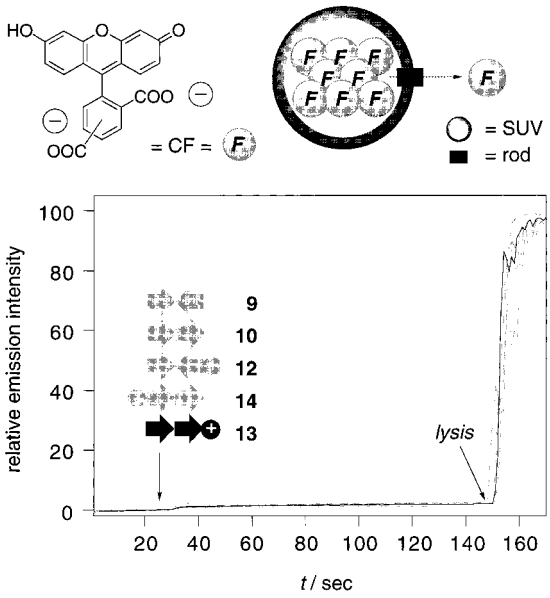

Figure 9. Assay for lytic activity of neutral and cationic rods in unpolarized bilayer membranes. Top, schematic representation of the assay. Bottom, changes in fluorescence intensity of intravesicular CF (50 mM) during the addition of rods (10 μM) and final lysis (excess Triton X-100). Relative emission intensity $= (I_t - I_0)/(I_\infty - I_0) \times 100\%$; $\lambda_{em} = 514$ nm, $\lambda_{ex} = 492$ nm. (Conditions: 0.25 mM EYPC-SUVs in 10 mM HEPES buffer, 107 mM NaCl).

In conclusion, general importance for cell membrane recognition was identified for (a) the interaction between the axial rod dipole and membrane potential and (b) the TM charge translocation but not for (c) the membrane surface charge and (d) the ion transport mechanism. Two findings were particularly noteworthy within a consistent set of data collected for several neutral and cationic rigid-rod ionophores of different electrostatic axial asymmetry. On the one hand, rigid push-pull rods with an electrostatic axial asymmetry similar to that of the α-helical bee toxin melittin showed an increased activity in polarized bilayer membranes that coincided with structural evidence for a favorable alignment of the axial rod dipole with potentials. Reduced activity of the isomeric rods with electrostatic axial asymmetry similar to that of natural antibiotics in polarized bilayers, on the other hand, was compellingly evidenced to originate from voltage-induced inhibition of rod incorporation into membranes with mammal-type polarization. These two findings provide, to the best of our knowledge, the first direct experimental evidence of the molecular structural level for operational cell membrane recognition by electrostatically asymmetric nanorods.[1,23]

Experimental Section

See Supporting Information.

Acknowledgment. We thank B. Ghebremariam, Dr. J.-Y. Winum, Dr. F. Robert, and S. Biltresse for synthetic assistance, A. Pinto and J.-P. Saulnier and the group of Prof. Gülaçar for NMR and MS, respectively, and Swiss NSF (21-57059.99) for financial support.

Supporting Information Available: Experimental procedures, RP-HPLC profiles for product mixtures **9**/**16**/**17**, **9**/**10**/**11** and **17**/**18**/**19**/**20** (Figure 10), vesicle preparation, flux assays, and single ion channel characteristics in planar bilayer conductance experiments (Figure 11). This material is available free of charge via the Internet at http://pubs.acs.org.

JA003141+

(23) Potential-induced translocation but not reorientation has been reported previously for asymmetric lantibiotic epilancin K7 rods: Driessen, A. J. M.; van den Hooven, H. W.; Kuiper, W.; van de Kamp, M.; Sahl, H.-G.; Konings, R. N. H.; Konings, W. N. *Biochemistry* **1995**, *34*, 1606−1614.